MSEG 410/610

Experimental Mechanics of Composite Materials

Lab 6: Quasi-Isotropic Laminate Tension and Notched Strength

Zachary Swain

Group Members

Chunyan Zhang

Evan Minnigh

Jerome Premkumar

Casey Busch

Performed on: May 1, 2019 Submitted on: May 14, 2019

Abstract

Objective:

The purpose of this lab was to predict and experimentally determine specific mechanical properties of a carbon fiber laminate. This was done by executing experimental tensile loading for various specimen hole sizes. This provided a better understanding of effective experimental composite material notch testing, the mechanical properties that can be obtained from such experiments, and how to use and analyze different property predictions.

Summary of Results:

Unnotched and notched samples of quasi-isotropic mechanical response, with varying hole diameters, undergo experimental tensile testing. The resulting modulus of the unnotched specimens is reported as 4.98 Msi, strength as 92.2 ksi, ultimate strain as 0.0196, and Poisson ratio of 0.34. For the notched samples, strength is reported as 76.6 ksi for 1/16”, 65.6 ksi for 1/8”, and 57.3 for 1/4” hole diameters. A characteristic d_o is found for each case, and a best-fit d_o is found to correlate to σ_n/σ_o data for each at 0.0425. Predictive properties are obtained utilizing Autodesk Helius, resulting in a predicted modulus of 5.57 Msi, and a predicted Poisson ratio of 3.13, which are seen to correlate well to the experimental data reported.

Procedure

ASTM Standard:

The panel was fabricated with a lay-up that will be described by nomenclature and notation as defined in ASTM D 6507. Tensile testing set up and operation of unnotched and notched specimens were executed in accordance with ASTM D 3039[1] and ASTM D 5766[2].

Specimen Lay-up and Geometries:

The quasi-isotropic laminate was fabricated with a $[45,0,-45,90]_s$ lay-up composed of G-83C resin and T700 carbon fiber prepreg.[3] Post-process machining was done to form four unnotched specimens, in their respective testing geometries. These specimens were used to investigate the short beam strength and flexural properties of the panel, and to compare to property prediction. Sampled and averaged specimen geometries can be found in Table 1.

Instrumentation:

Instron 5985 and Instron 8562 tensile test setups was used for unnotched and notched specimens, respectively. Bluehill software suite was used to control and record data measurement. Microsoft Excel was utilized for data reduction purposes.

Instron Settings:

Tensile tests were operated on the Instron 5985 with a 250kN load cell, and the 8562 with a 100kN load cell. Specimens were loaded at a constant 0.05 in/min crosshead rate for all specimens and spans. Instron input was modulated by the Bluehill software suite.

Testing Environment:

Testing was done in University of Delaware's Center for Composite Materials, inside a controlled test lab. Appropriate safety equipment was worn. Humidity and ambient temperature levels were not closely monitored.

Results

Data Reduction Scheme:

Load and Strain data obtained for each unnotched specimen tested were recorded and exported to excel. Load and displacement data were similarly recorded for notched specimens. This data was used to generate stress-strain curves for the unnotched case to characterize the mechanical response of the specimen. Once the slope became linear, the slope was taken and recorded as modulus. The maximum force encountered before failure was likewise recorded for both sample categories. These stress values were both averaged for each hole size and reported as strength, and strain at break was likewise recorded. Poisson ratio is found by relating the strain results of each grid of the strain gage.

Nondimensionalized σ_n/σ_o is found over varying hole diameters, by equations presented below. Likewise, the ratio of KT/KT_inf is calculated at each diameter and found to be reasonably close to 1. A characteristic length d_o is also found using an equation detailed later, found for each diameter, and averaged. A best-fit d_o is found to match the results of the σ_n/σ_o results.

Tables:

Hole D, Specimen	Thickness (in)	Width (in)	CSA (in^2)
0 #1	0.150	1.002	0.150
0 #2	0.153	1.002	0.154
0 #3	0.151	1.001	0.151
0 #4	0.150	1.001	0.150
.25 #1	0.146	1.496	0.219
.25 #2	0.152	1.496	0.227
.25 #3	0.150	1.496	0.225
.0625 #4	0.151	1.499	0.227
.0625 #5	0.151	1.500	0.226
.0625 #6	0.152	1.498	0.228
.125 #7	0.154	1.505	0.232
.125 #8	0.150	1.505	0.226
.125 #9	0.149	1.475	0.219

Table 1: Sampled and averaged specimen dimensions

Specimen	Modulus (psi)	Ult. Strength (psi)	Ult. Strain	Poisson
1	4835282	86487	0.0197	0.3218
2	5123136	94118	0.0191	0.3596
3	4997300	95708	0.0196	0.3404
4	4979072	92511	0.0198	0.3437
avg	**4983698**	**92206**	**0.0196**	**0.3414**

Table 2: Unnotched tensile specimens' Modulus, Strength, Strain-to-failure, and Poisson ratio are calculated.

Specimen	1	2	3	4	5	6	7	8	9
Hole D (in)	0.25	0.25	0.25	0.0625	0.0625	0.0625	0.125	0.125	0.125
Max Load (lb)	12335.2	13203.6	12921.0	17748.4	17322.8	17023.0	15159.5	14981.4	14276.8
Max Stress (psi)	56296.0	58116.8	57490.7	78351.2	76666.5	74778.3	65315.7	66215.6	65135.6

Table 3: Maximum load is reported for each notched specimen, and maximum stress is calculated.

Hole D	0.0625	0.125	0.25
Avg Strength	76599	65556	57301
KT/KT_inf	1.0018	1.0074	1.0315
do (in)	0.0194	0.0389	0.0778

Avg do	0.0454

Table 4: Average strength of each hole size is calculated from the max stresses calculated, KT/KT_inf and do are reported for each hole size.

Hole D	1/KT_inf	σn/σo	1-(D/W)	D/W	R	best fit do σn/σo
0	0.333333	1	1	0	0	1
0.0625	0.333333	0.830734	0.958333	0.041667	0.03125	0.878635594
0.125	0.333333	0.710969	0.916667	0.083333	0.0625	0.732356159
0.25	0.333333	0.621447	0.833333	0.166667	0.125	0.57349541

best fit do	do=.0425

Table 5: σn/σo, lower and upper bounds, and a best fit do are calculated.

Graphs of Stress-Strain Data:

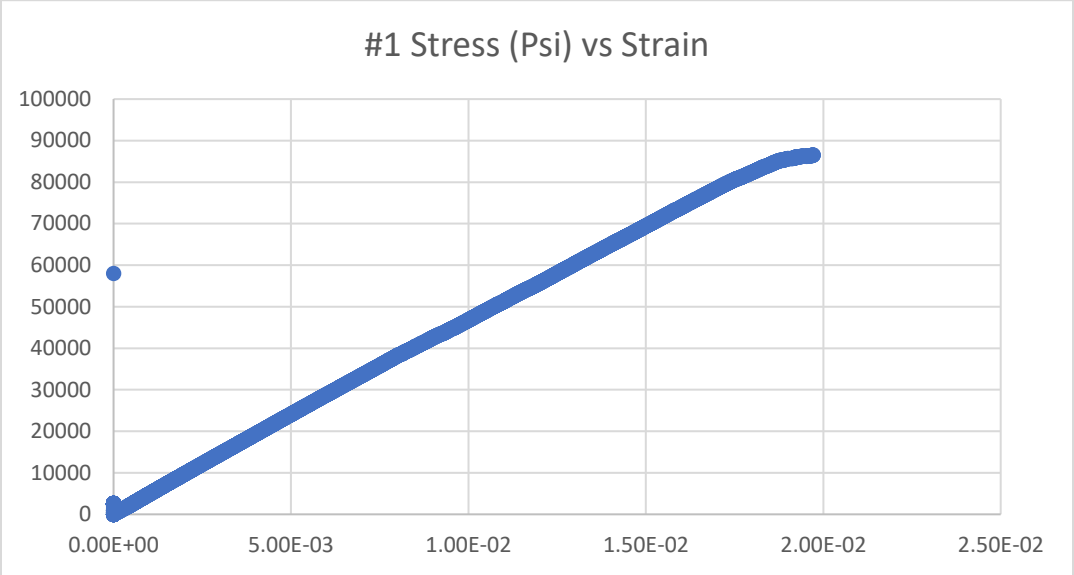

Fig 1: Stress-strain curve of unnotched specimen #1.

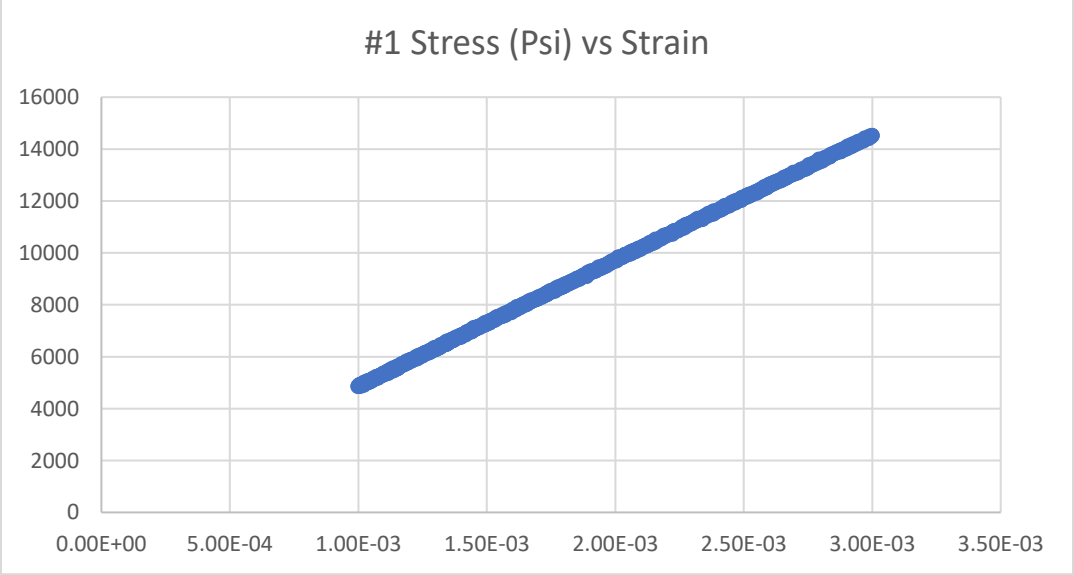

Fig 2: Stress-strain curve from Strain= 0.001 to 0.003 for modulus calculation of unnotched specimen #1.

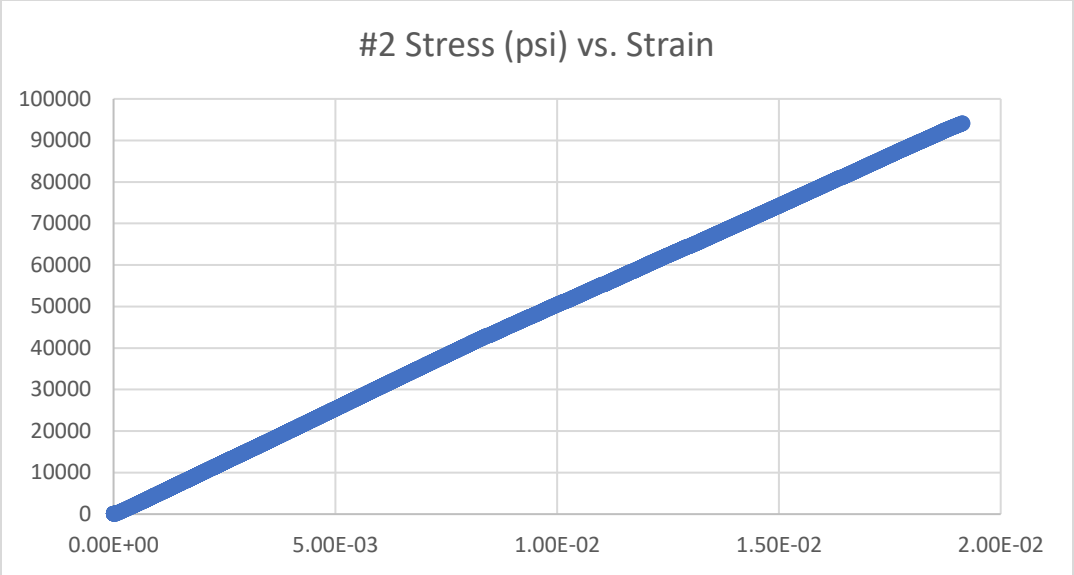

Fig 3: Stress-strain curve of unnotched specimen #2.

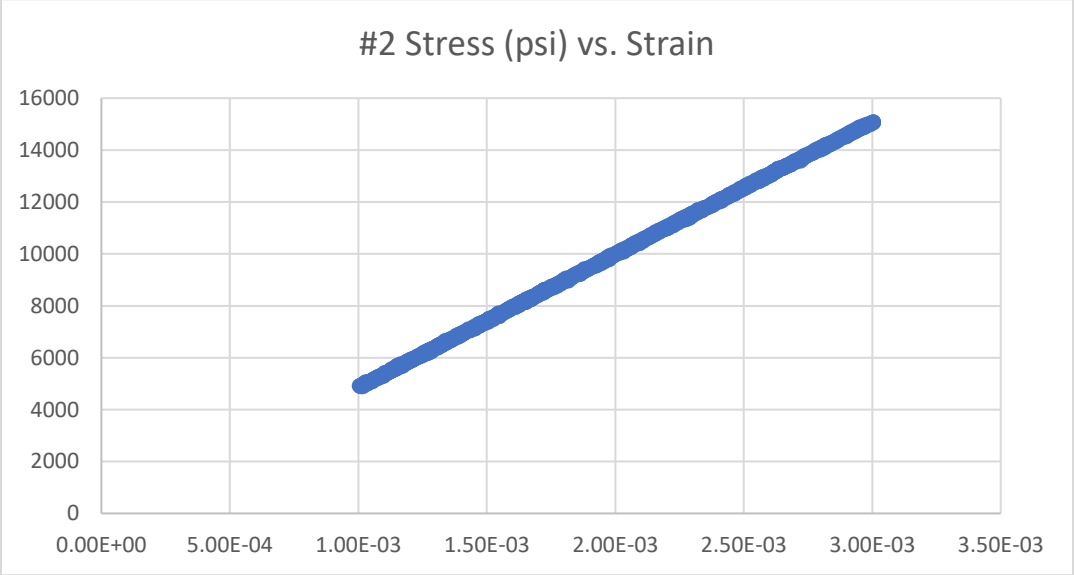

Fig 4: Stress-strain curve from Strain= 0.001 to 0.003 for modulus calculation of unnotched specimen #2.

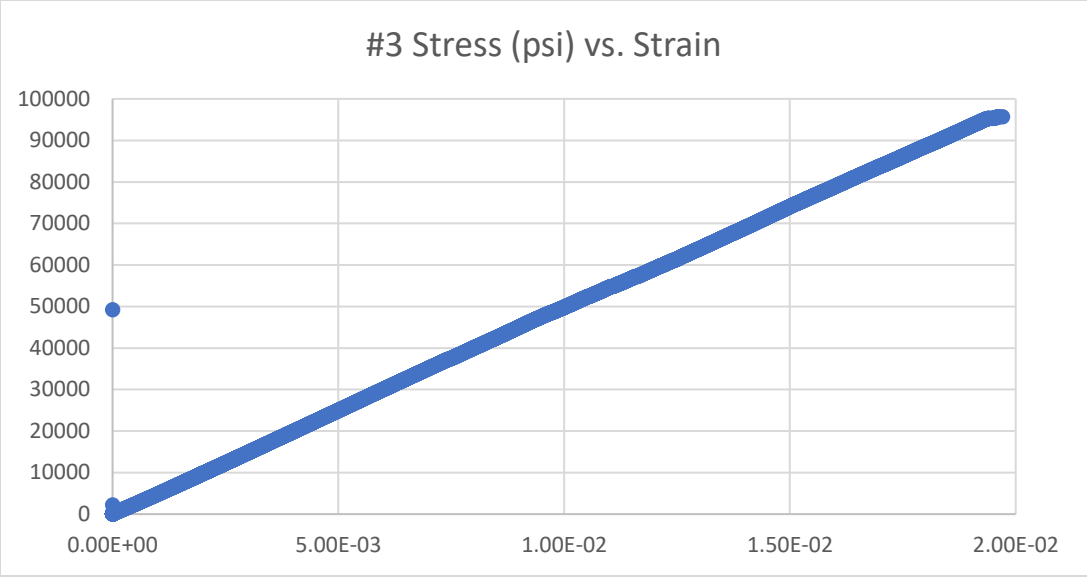

Fig 5: Stress-strain curve of unnotched specimen #3.

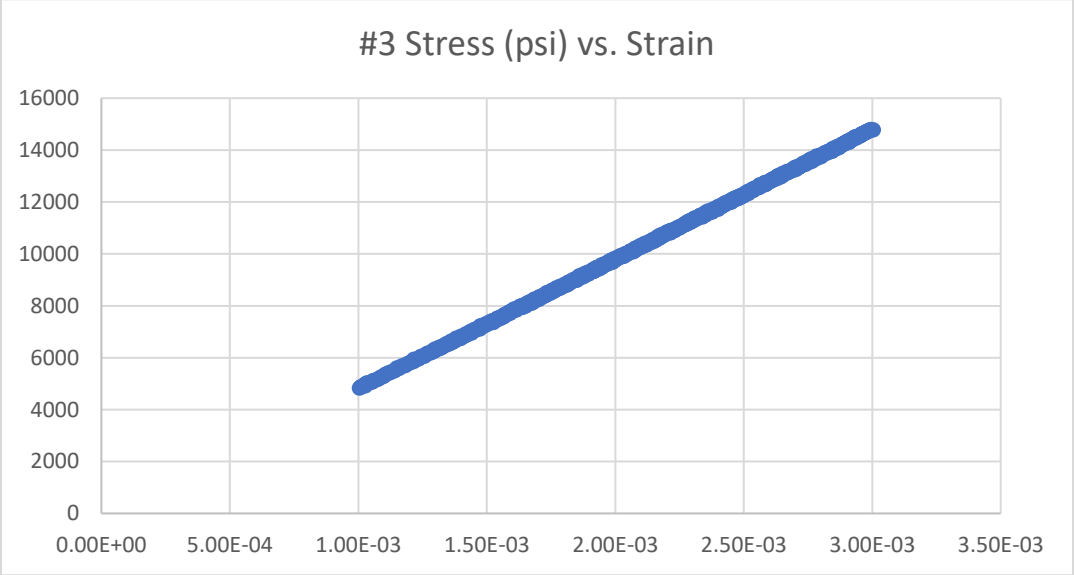

Fig 6: Stress-strain curve from Strain= 0.001 to 0.003 for modulus calculation of unnotched specimen #3.

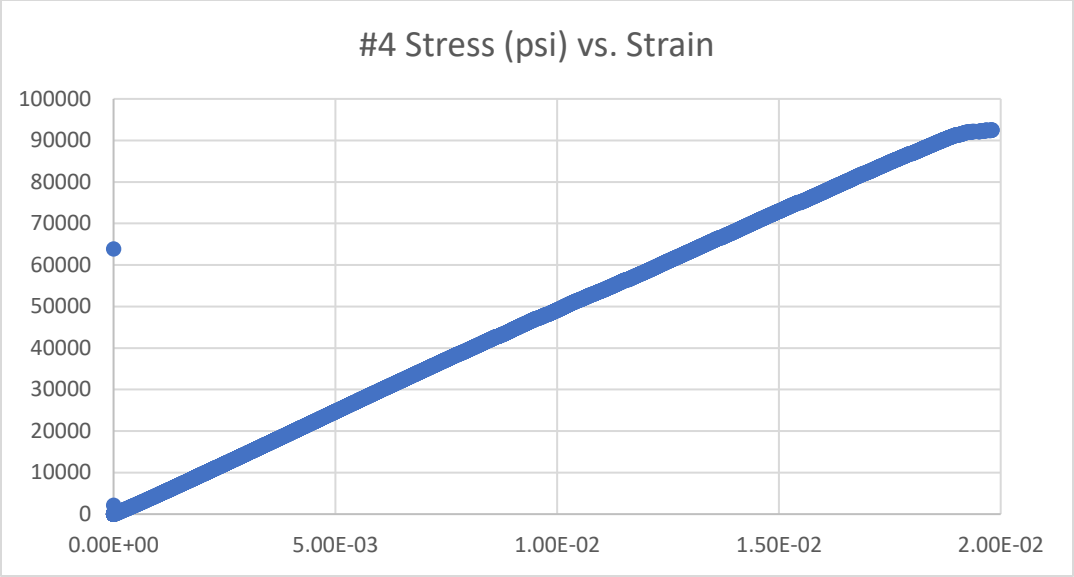

Fig 7: Stress-strain curve of unnotched specimen #4.

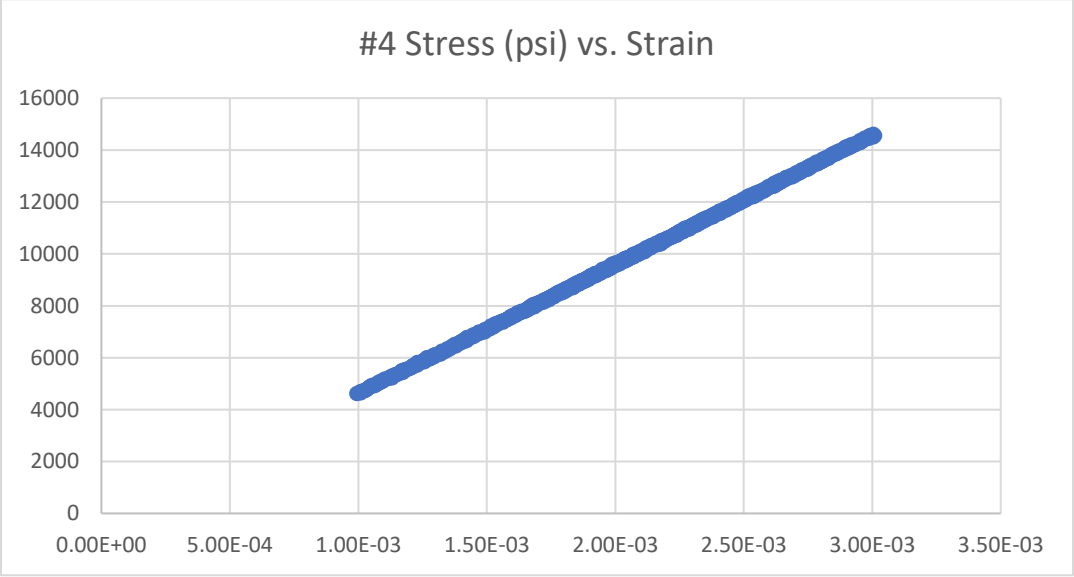

Fig 8: Stress-strain curve from Strain= 0.001 to 0.003 for modulus calculation of unnotched specimen #4.

***Equations*:**

$$\sigma_y(x,0) = \frac{\sigma^\infty}{2}\left\{2 + \left(\frac{R}{x}\right)^2 + 3\left(\frac{R}{x}\right)^4 - \left(K_T^\infty - 3\right)\left[5\left(\frac{R}{x}\right)^6 - 7\left(\frac{R}{x}\right)^8\right]\right\}; x > R \tag{1}$$

$$\frac{\sigma_y}{\sigma^\infty} = 1 + \frac{1}{2}\left(\frac{R}{x}\right)^2 + \frac{3}{2}\left(\frac{R}{x}\right)^4 \tag{2}$$

$$\frac{K_T}{K_T^\infty} = \frac{2 + (1 - (D/w))^3}{3(1 - (D/w))} \tag{3}$$

$$\frac{\sigma_N^\infty}{\sigma_o} = \frac{2}{\left[2 + \xi_1^2 + 3\xi_1^4 - \left(K_T^\infty - 3\right)\left(5\xi_1^6 - 7\xi_1^8\right)\right]}$$

$$\xi_1 = \frac{R}{R + d_o} \tag{4}$$

***Summary of Test Results*:**

A series of unnotched and notched samples – at varying hole diameters – are tested experimentally under tensile loading. Modulus of the unnotched specimens is reported as 4.98 Msi, strength as 92.2 ksi, ultimate strain as 0.0196, and Poisson ratio of 0.34. For the notched samples, strength is reported as 76.6 ksi for 1/16", 65.6 ksi for 1/8", and 57.3 for ¼". A characteristic d_o is found for each case, and a best-fit d_o is found to correlate to σ_n/σ_o data for each.

Poisson ratio is calculated for each of the unnotched samples tested, and averaged to find the above value. This was done by utilizing a biaxial strain gage during testing and forming a ratio of longitudinal to transverse strain. Below are figures of strain plotted against each grid to find this slope.

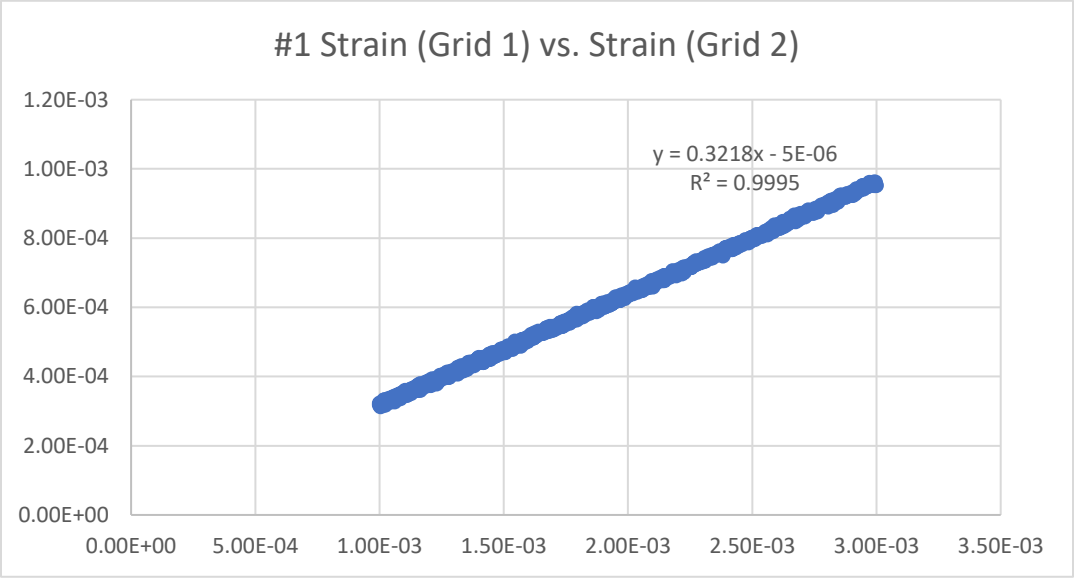

Fig 9: Strain grid curve for Poisson ratio calculation of unnotched specimen #1.

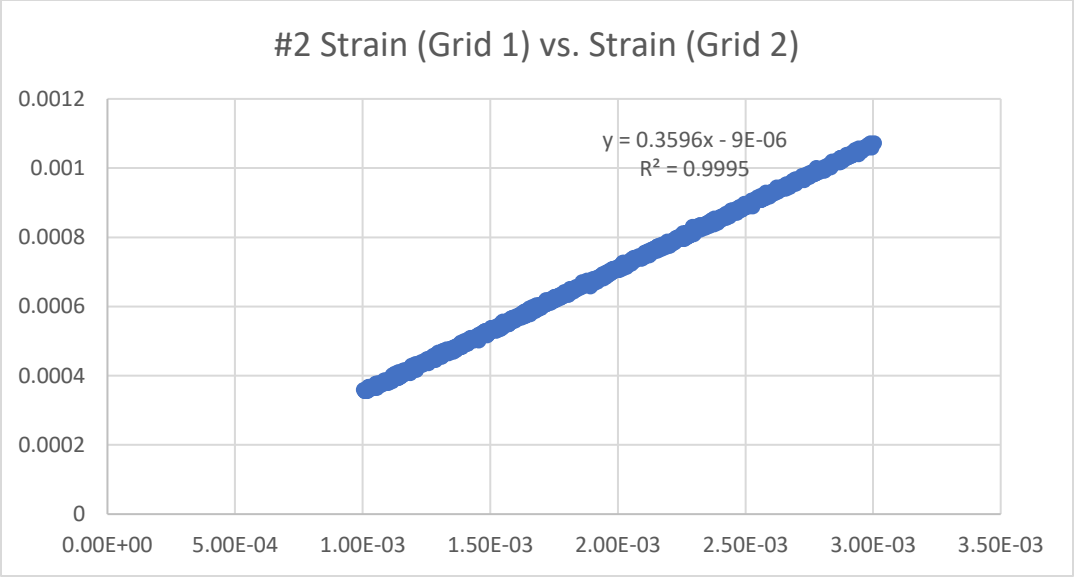

Fig 10: Strain grid curve for Poisson ratio calculation of unnotched specimen #2.

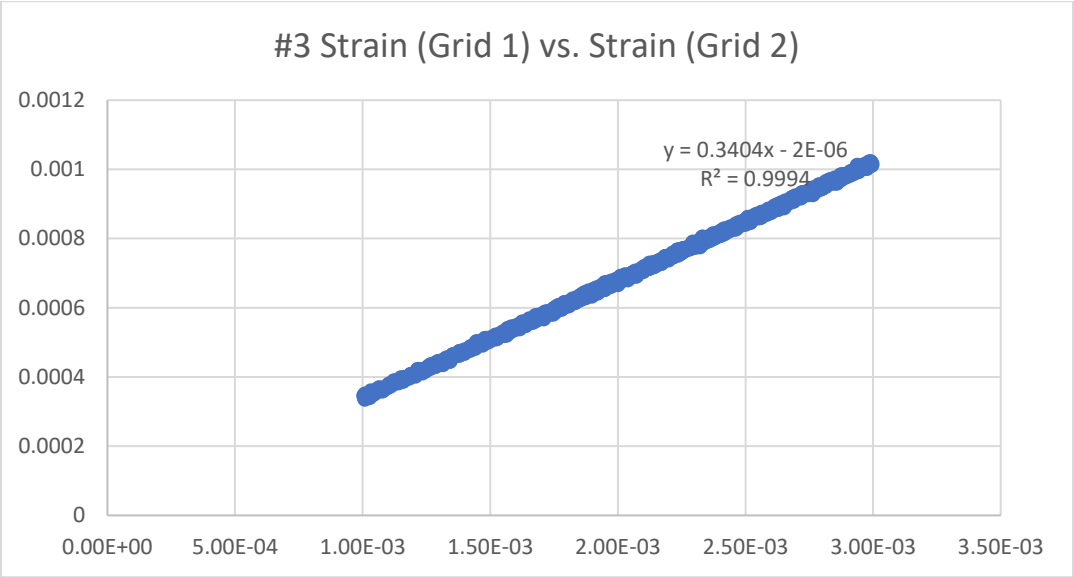

Fig 11: Strain grid curve for Poisson ratio calculation of unnotched specimen #3.

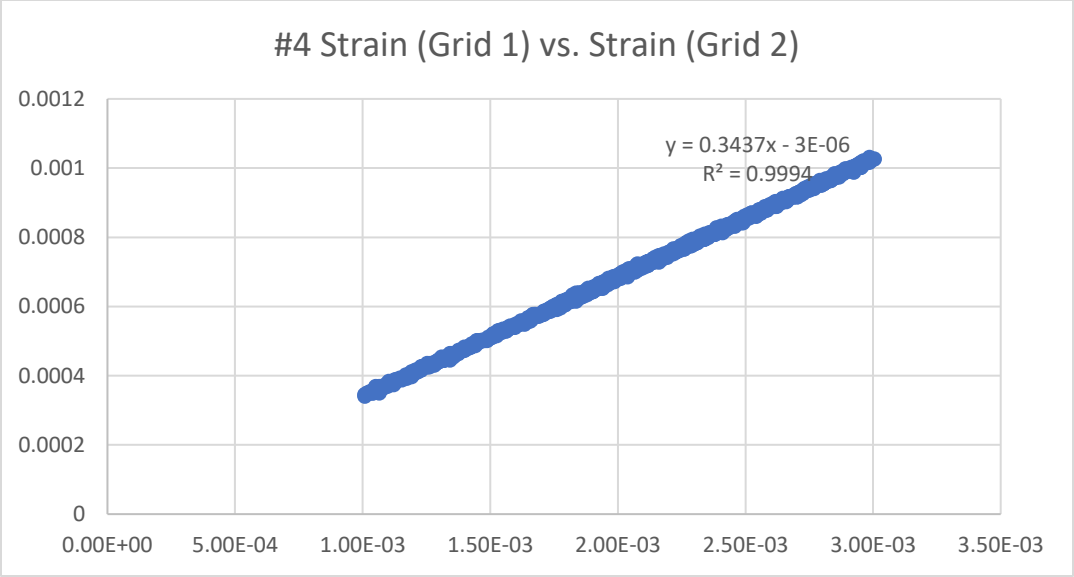

Fig 12: Strain grid curve for Poisson ratio calculation of unnotched specimen #4.

A nondimensionalized σ_y/σ is plotted against increasing values of X+R from the edge of the hole, using equation 2. It is shown that for decreasing hole size, the stress concentration dissipates over a smaller X+R distance. This expanded range of stress concentration for larger hole sizes interacts with a larger volume of the sample, over which there may be defects. This corresponds to a lower strength being associated with larger hole sizes.

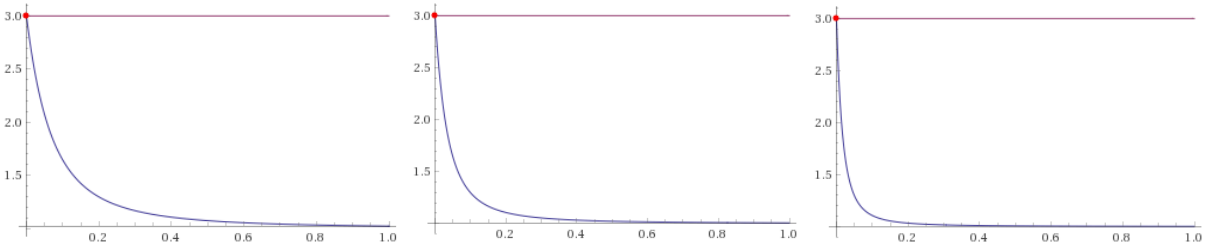

D=.25 D=.125 D=.0625

Fig 13: Value of concentrated to far field stress is plotted over varying hole diameters.

KT/KT_inf is calculated by geometric relations detailed in equation 3. These results are presented above in Table 4. KT_inf is known to be 3 for infinitely wide samples, and as such, KT can be solved for using specimen geometry. Below are the corresponding KT values for each hole diameter.

Hole D	**0.0625**	**0.125**	**0.25**
KT	3.0054	3.0221	3.0944

Table 6: KT is calculated over varying hole diameter.

Nondimensionalized σ_n/σ_o is plotted over varying radii of holes. Below, results are presented that depict a decreasing notch strength for increasing hole radius. These ratios are then plotted against D/W and upper and lower bounds of 1-(D/W) and 1/KT_inf are respectively applied. The data falls smoothly in between its logical bounds, as shown below.

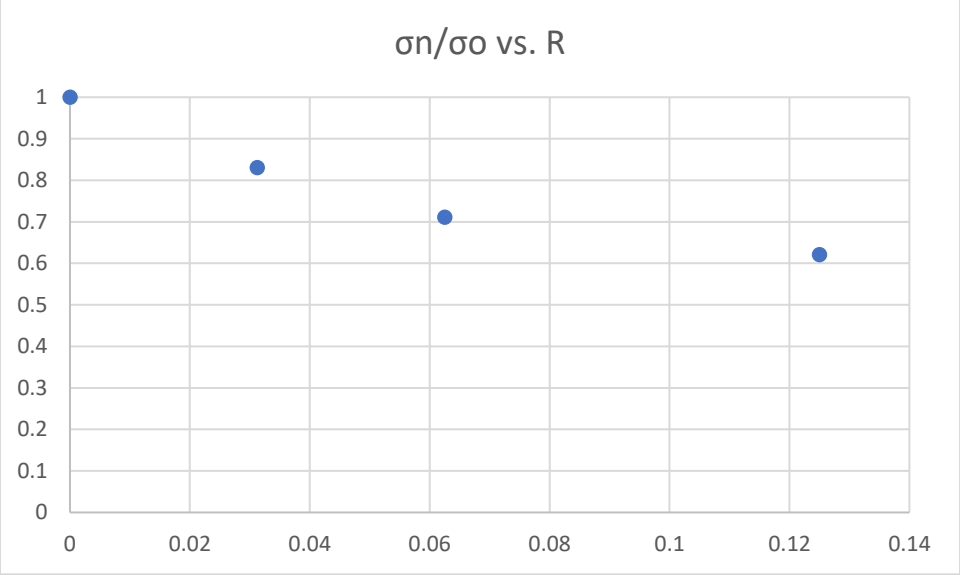

Fig 14: Ratio of σn/σo vs. R is plotted over increasing hole radius.

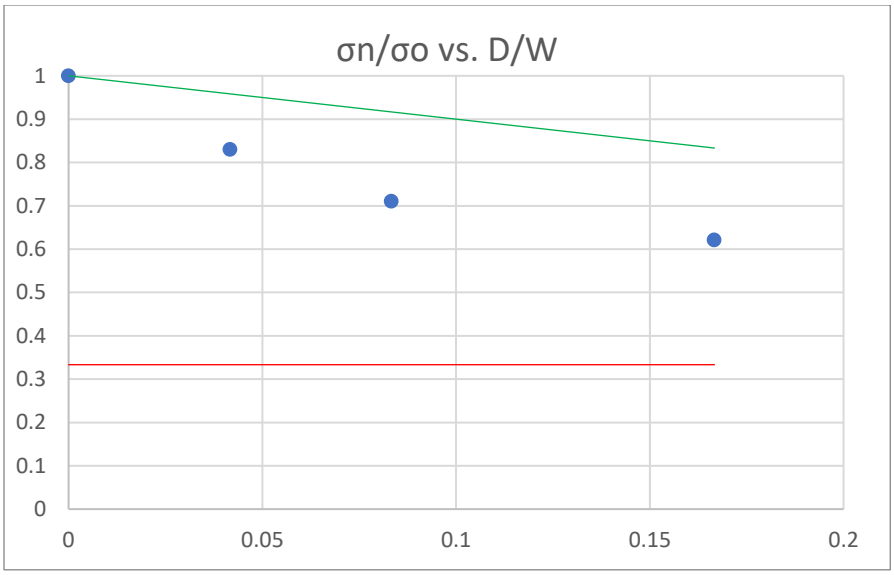

Fig 15: Ratio of σn/σo vs. R is plotted over increasing hole diameter to specimen width. Upper and lower bounds are applied as described.

Values of d_o are calculated as per equation 4. For known notch strength, unnotched strength, hole radius and KT_inf, values of d_o are found for varying hole diameter. These values are averaged and found to be 0.0454 as reported above in Table 4. A best-fit value of d_o is then found by variation to match best the σ_n/σ_o results. A best-fit value was found as d_o=0.0425. This correlation is shown below.

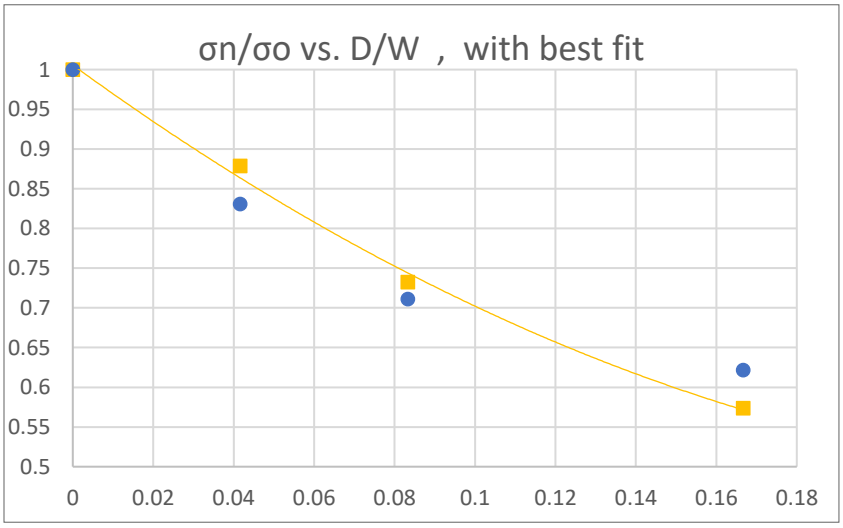

Fig 16: Best-fit trendline of σn/σo using modified d_o is compared to σn/σo data.

Description of Failure Modes:

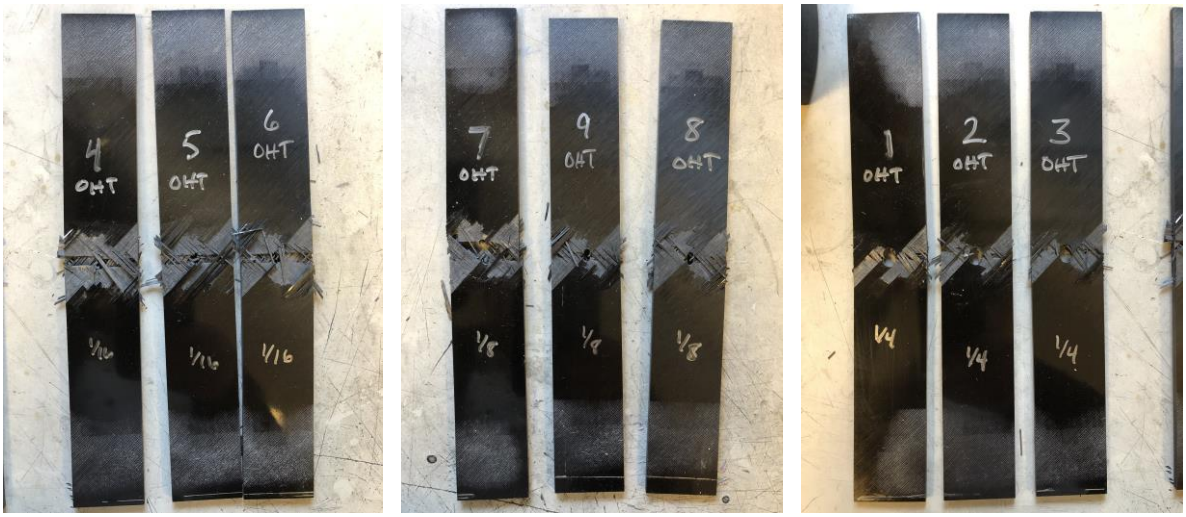

Fig. 17: Failed samples are images over varying hole diameters.

Failure modes of each hole size are seen to fail transverse to the loading direction, through the midsection of the hole. Splitting and 45° fiber fray is seen across each hole diameter. Audible cracking was observed during testing, as well as explosive failure.

Correlation of Theory and Experiments

Samples are seen to fail at the midsection of the hole for varying hole diameters across all hole sizes measured. This is due to the stress concentration imparted by the drilled-out section not being present to equally distribute the load over its cross section. The resultant stress concentration seen to dissipate over increasing X+R, but is dissipated over a greater distance (greater do) for larger hole diameters. Creating a larger volume of specimen proximate to the hole that maintains a higher stress concentration, these larger holes also provide for more

opportunity for defects to interact with this elevated stress concentration and lead to failure. The specimens tested with larger holes were seen to have lesser tensile strength, accordingly.

Conclusions

A series of unnotched and notched samples of varying hole diameters are experimentally tested under tensile loading. The resulting modulus of the unnotched specimens is reported as 4.98 Msi, strength as 92.2 ksi, ultimate strain as 0.0196, and Poisson ratio of 0.34. For the notched samples, strength is reported as 76.6 ksi for 1/16", 65.6 ksi for 1/8", and 57.3 for ¼". A characteristic d_o is found for each case, and a best-fit d_o is found to correlate to σ_n/σ_o data for each. Predictive properties are obtained utilizing Autodesk Helius, resulting in a predicted modulus of 5.57 Msi, and a predicted Poisson ratio of 3.13. These are seen to correlate well to the experimental data reported, and future work with the software will facilitate better acustomization to its utility, and will provide clarity to unknown facets encountered.

References

[1] ASTM Standard D3039, “Standard Test Method for Tensile Properties of Polymer Matrix Composite Materials,” ASTM International, West Conshohocken, PA, 2003, www.astm.org/Standards/D3039.htm

[2] ASTM Standard D5766, “Standard Test Method for Open-Hole Tensile Strength of Polymer Matrix Composite Laminates,” ASTM International, West Conshohocken, PA, 2003, www.astm.org/Standards/D5766.htm

[3] T700S Data Sheet [PDF]. Santa Ana, CA: Toray Carbon Fibers America Inc. https://www.toraycma.com/file_viewer.php?id=4459.

Appendix A

Autodesk Helius is used to predict mechanical properties and failure sequencing and modes. Ply properties are input to simulate that of the T700-G83C prepreg being used in experiment, and then 8 plies are stacked in the sequence described above as $[45,0,-45,90]_s$. An axial load is then applied, large enough to promote failure of each ply. Stressing and straining steps are then calculated as prescribed by the relation of chosen amount of data points to applied stress. For Max Stress failure criteria, an individual ply will fail when it reaches the ultimate strength for that respective orientation to tensile loading. A predictive plot is generated by interpolating the results generated for each of these steps. A plot and failure data of the applied Max Stress criteria is given below. It is unknown why the plot continues gathering data points after all plies have failed; upon inspection of the failure steps, it is noticed that the last plies fail at ~0.0169 strain, but the plot continues gathering increasing stress far beyond this. This is judged to be an anomaly of the software itself – or at least with the implementation of it. Other students were verified to have experienced the same issue. Data past the 8^{th} failing ply is judged to be erroneous, as the plot should drop off significantly past this point.

Ply properties are input as the email-provided values, supplemented by similar T700 ply properties defaulted in the software. Failure sequencing are seen to be predicted first-to-last as 90, 45, 0 in failure modes of transverse, shear, and longitudinal failures respectively. Modulus is obtained from the results of the simulation by sampling and calculating the ratio of σ_x/ε_x at steps that were calculated. The same technique was used to find the Poisson ratio from the results of the simulation by taking longitudinal over the negative of transverse strains. The values of

both the computed modulus and that of the computed Poisson ratio are also provided below. Tsai-Wu Failure criteria is also used, with a parameter of -0.5. The plot is generated in a similar way as described above, and is provided below. The same method is undertaken to compute predictive modulus and Poisson ratio – the results of which are again reported below. The resulting moduli and Poisson ratios from these methods of predictive failure are quite close in value and when averaged, the software-predicted modulus and Poisson will be reported as 5.57 Msi. and 3.13, respectively. These results are seen to correlate well with the experimental data obtained in this lab.

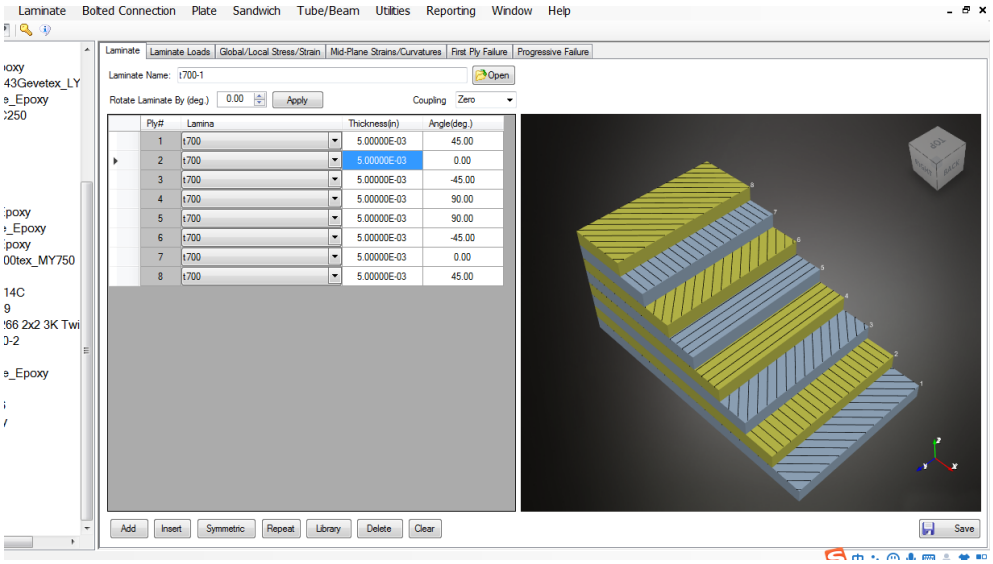

Fig. 18: Ply geometry is shown in stacking sequence of the laminate.

Title	Value
Composite Type	Unidirectional
Fiber Vf	5.40000E-01
Thickness (in)	5.00000E-03
E11 (psi)	1.55000E+07
E22 (psi)	1.00000E+06
E33 (psi)	1.00000E+06
G12 (psi)	3.50000E+05
G13 (psi)	3.50000E+05
G23 (psi)	3.10000E+05
NU12	3.17000E-01
NU13	3.17000E-01
NU23	3.64000E-01
CTE1 (in/in/F)	1.58000E-07
CTE2 (in/in/F)	1.04600E-05
CTE3 (in/in/F)	1.04600E-05
CME1 (in/in/%m)	0.00000E+00
CME2 (in/in/%m)	0.00000E+00
CME3 (in/in/%m)	0.00000E+00
+S1 (psi)	2.53000E+05
+S2 (psi)	5.30000E+04
-S1 (psi)	-8.80000E+04

Title	Value
NU23	3.64000E-01
CTE1 (in/in/F)	1.58000E-07
CTE2 (in/in/F)	1.04600E-05
CTE3 (in/in/F)	1.04600E-05
CME1 (in/in/%m)	0.00000E+00
CME2 (in/in/%m)	0.00000E+00
CME3 (in/in/%m)	0.00000E+00
+S1 (psi)	2.53000E+05
+S2 (psi)	5.30000E+04
-S1 (psi)	-8.80000E+04
-S2 (psi)	-2.47000E+04
S12 (psi)	6.90000E+04
+e1 (in/in)	1.68000E-02
+e2 (in/in)	2.78000E-03
-e1 (in/in)	5.78000E-03
-e2 (in/in)	1.62000E-02
e12 (in/in)	4.50000E-03
K1 (Btu/hr/ft/F)	0.00000E+00
K2 (Btu/hr/ft/F)	0.00000E+00
K3 (Btu/hr/ft/F)	0.00000E+00
Density (lb/in3)	5.60000E-02

Fig. 19: Ply properties are reported as used. Properties were obtained as given values, and supplemented by similar default

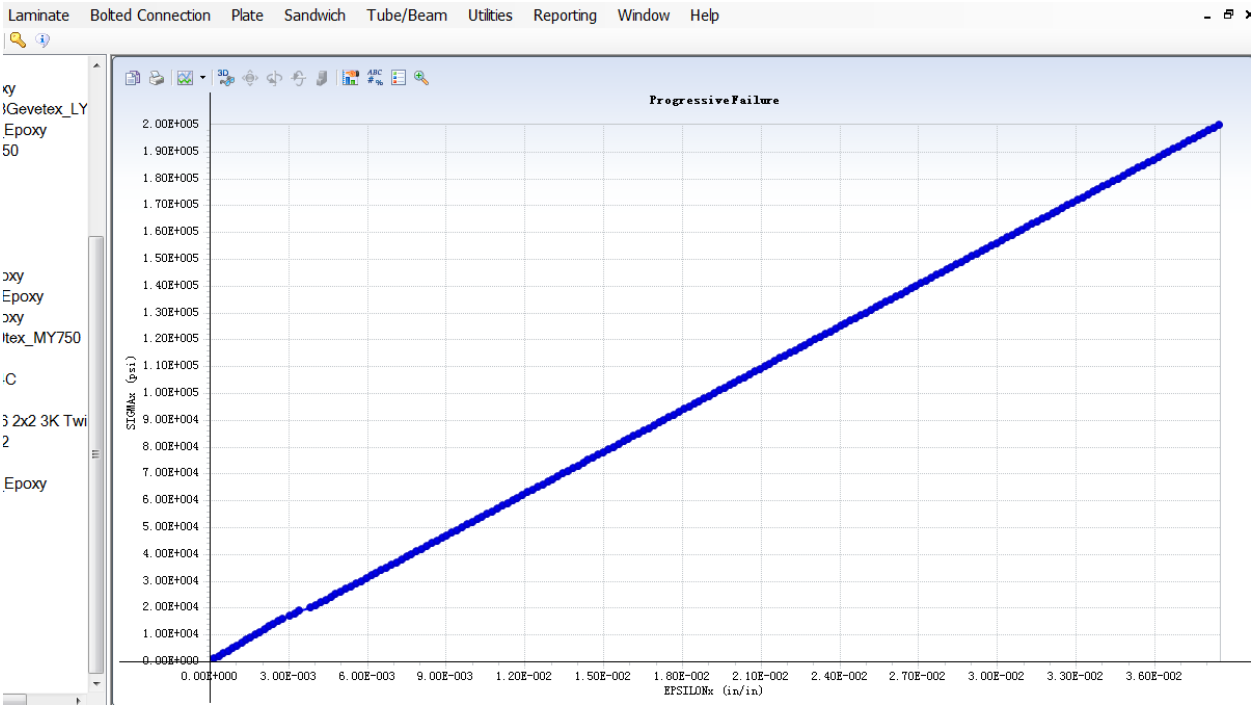

Fig. 20: Predictive Max stress criteria stress-strain plot generated from the software. Points are interpolated between calculated steps.

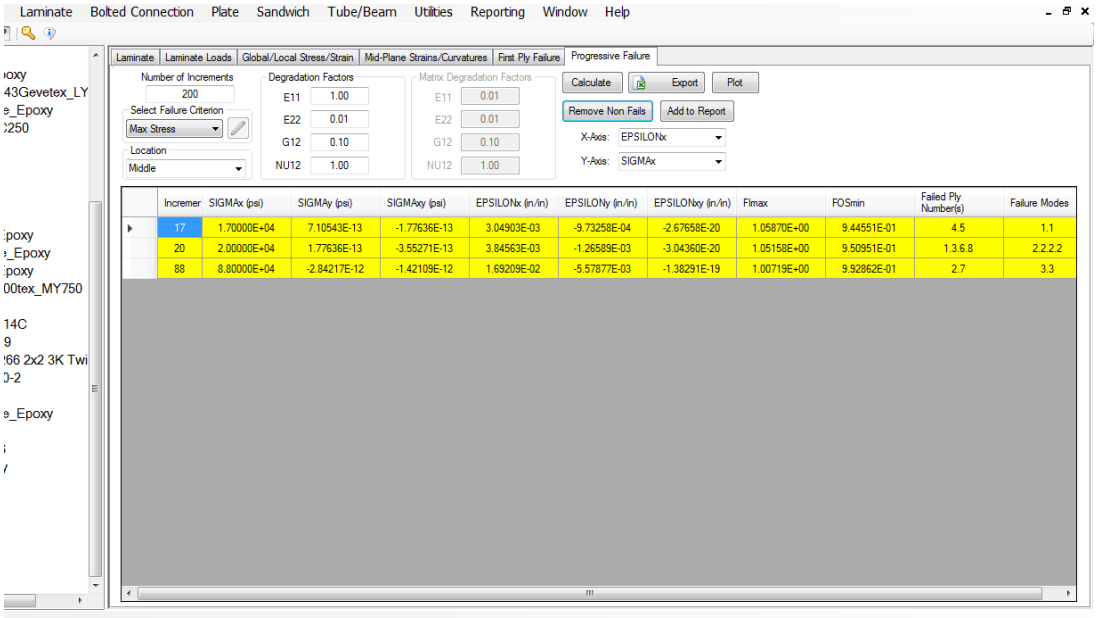

Fig. 21: Failure steps are shown for Max stress criteria. Ply failure sequencing is shown, along with respective modes

Modulus	Poisson
5575598	3.1326

Table 7: Max Stress criteria predicted modulus and Poisson ratio are reported.

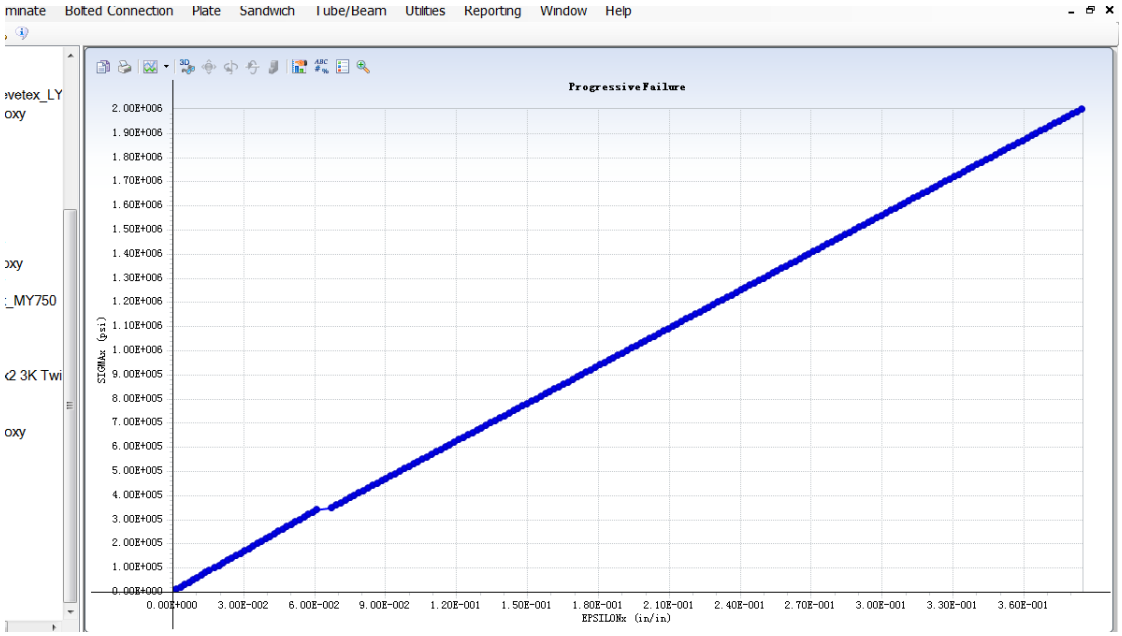

Fig. 22: Predictive Tsai-Wu criteria stress-strain plot generated from the software. Points are interpolated between calculated steps.

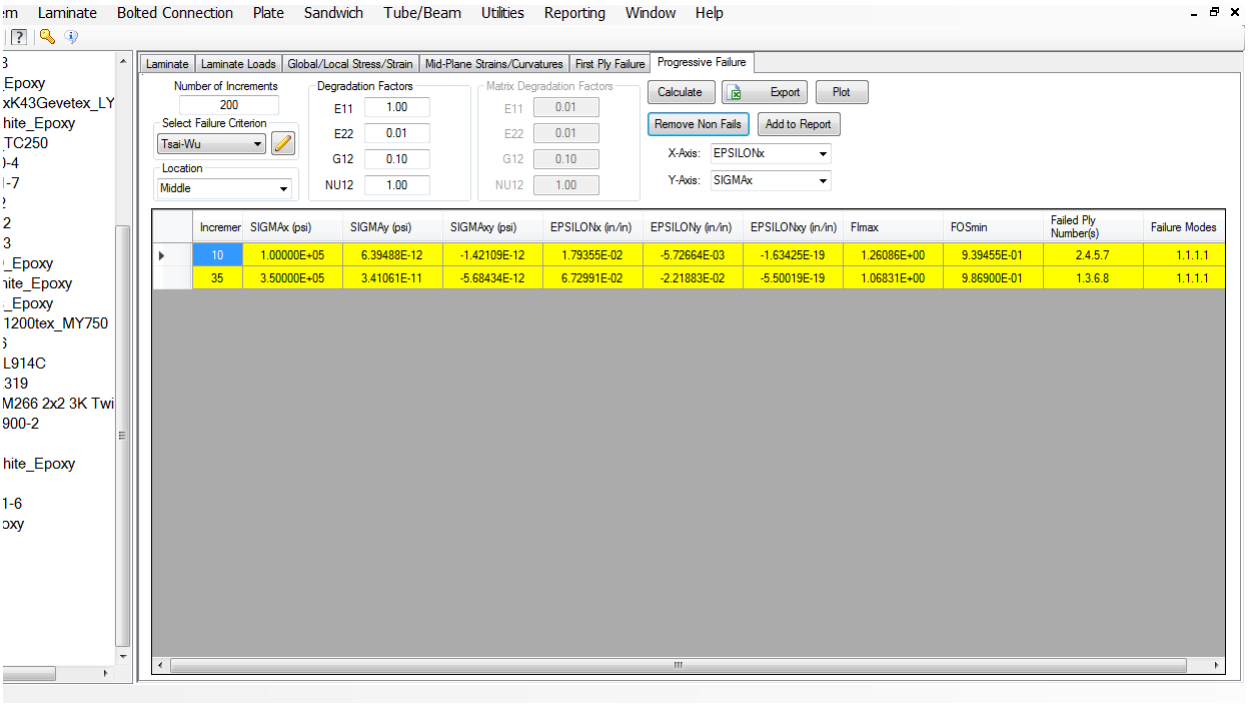

Fig. 23: Failure steps are shown for Tsai-Wu criteria. Ply failure sequencing is shown, along with respective modes. These failure modes are dismissed in favor of those by Max Stress, as they are more intuitively logical predictions.

Modulus	Poisson
5574136	3.1331

Table 8: Tsai-Wu criteria predicted modulus and Poisson ratio are reported.

Supplemental

All files used in calculation are available at https://github.com/zswain/MSEG610